Food & Function

Accepted Manuscript

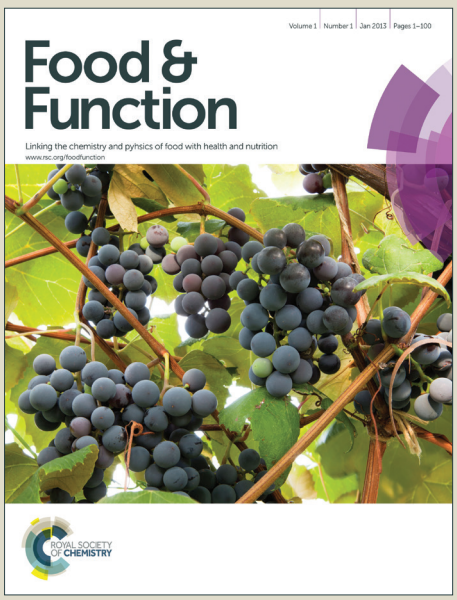

This is an *Accepted Manuscript*, which has been through the Royal Society of Chemistry peer review process and has been accepted for publication.

Accepted Manuscripts are published online shortly after acceptance, before technical editing, formatting and proof reading. Using this free service, authors can make their results available to the community, in citable form, before we publish the edited article. We will replace this *Accepted Manuscript* with the edited and formatted *Advance Article* as soon as it is available.

You can find more information about *Accepted Manuscripts* in the Information for Authors.

Please note that technical editing may introduce minor changes to the text and/or graphics, which may alter content. The journal's standard Terms & Conditions and the Ethical guidelines still apply. In no event shall the Royal Society of Chemistry be held responsible for any errors or omissions in this *Accepted Manuscript* or any consequences arising from the use of any information it contains.

ROYAL SOCIETY OF CHEMISTRY

www.rsc.org/foodfunction

Ginkgo biloba extract (Egb761) attenuates zinc-induced tau phosphorylation at Ser262 by regulating GSK3β activity in rat primary cortical neurons

Kyoung Ja Kwon[1,2], Eun Joo Lee[1], Kyu Suk Cho[1], Du-Hyong Cho[3], Chan Young Shin[1] and Seol-Heui Han[1,2*]

[1]Department of Neuroscience, Center for Neuroscience Research, Institute of Biomedical Science and Technology, Konkuk University School of Medicine, [2]Department of Neurology, Konkuk University Medical Center, 120 Neungdong-ro Gwangjin-gu, Seoul 143-701, Korea

[3]Department of Pharmacology, School of Medicine, Eulji University, 77, Gyeryong-ro, 771 Beon-gil, Jung-gu, Daejeon 301-746, Korea

Running title: Egb761 inhibits tau hyperphosphorylation

* Corresponding author: Seol-Heui Han

Seol-Heui Han

Department of Neurology, Konkuk University School of Medicine and Konkuk University Medical Center,

120 Neungdong-ro, Gwangjin-gu, Seoul, 143-701, Korea

Tel) ±82-2-454-5630; Fax) ±82-2-2030-7899; E-mail) alzdoc@naver.com

Abstract

In the brain, the excessive amount of zinc promotes the deposition of β-amyloid proteins and the intraneuronal accumulation of neurofibrillary tangles composed of hyperphosphorylated tau proteins. These consequences are key neuropathological traits that reflect Alzheimer's disease. Egb761, a standardized *Ginkgo biloba* extract, is a powerful antioxidant known to exhibit neuroprotective actions. In this study, we investigated whether Egb761 can counteract the zinc-induced tau phosphorylation in rat primary cortical neurons. To determine the modification of tau phosphorylation by Egb761 treatment, we conducted Western blot analyses, MTT assay, ROS measurement and immunocytochemistry. We found that zinc-induced tau phosphorylation occurred at Ser262 in a time- and dose-dependent manner while other tau sites were not phosphorylated. Tau phosphorylation at Ser262 was increased 30 min and peaked 3 h after zinc treatment (control: 100 ± 1.2%, 30 min: 253 ± 2.24%, 3 h: 373 ± 1.3%). Interestingly, Egb761 treatment attenuated the zinc-induced tau hyperphosphorylation at Ser262 in a concentration-dependent manner while the antioxidant N-acetylcysteine showed a similar effect. Furthermore, Egb761 prevented the zinc-induced activation of p38 MAPK and GSK3β, as well as the zinc-induced increase in ROS production and neuronal cell death. Lithium chloride also inhibited the zinc-induced tau phosphorylation but did not affect ROS levels. These results suggest the potential of Egb761 in inhibiting the zinc-induced tau phosphorylation at Ser262 through its anti-oxidative actions involving the regulation of GSK3β. Therefore, Egb761 may be a candidate for the treatment of tauopathy present in neurological disorders such as Alzheimer's disease.

Key words: Tau phosphorylation, Reactive oxygen species, GSK3β, Tauopathy

Introduction

With the aging population, the prevalence of Alzeheimer's disease is increasing but the availability of treatment regimens are relatively lacking. The two key neuropathological hallmarks of AD are intracellular neurofibrillary tangles (NFTs) and extracellular amyloid plaques. NFTs are composed of abnormally hyperphosphorylated tau, a microtubule-associated protein[1, 2] which produces insoluble paired helical filaments. Tau is involved in the assembly and maintenance of microtubules, and its physiological function is modulated by phosphorylation. Tau is composed of 85 putative phosphorylation sites, nine of which are known to be phosphorylated in normal adult human brain[3-5]. Tau is hyperphosphorylated in many neurodegenerative diseases, as in AD[6], resulting to the formation of NFTs.

Extensive research on the signaling molecules leading to tau hyperphosphorylation found that tau can be phosphorylated by several protein kinases including cyclin-dependent kinase 5 (CDK5), glycogen synthase kinase 3β (GSK3β), mitogen-activated protein kinases (MAPKs) such as p38, and protein phosphatases such as PP2A[7-10]. Among these tau kinases and tau phosphatases, little is known about the role of MAPKs especially p38, on tau hyperphosphorylation. Some studies have reported that tau hyperphosphorylation activates SAPK/p38 [11, 12] and p38 MAPK phosphorylates tau at Thr181, Ser202, Thr205, Ser396, Ser404, and Ser422 in NFTs [13], and p38 MAPK activation increases tau phosphorylation at Ser396 and Ser404 [9]. Forty-five phosphorylated sites have been identified in brains with AD. Among these phosphorylation sites, at least 30 Ser/Thr are phosphorylated in NFTs. Many *in vivo* and *in vitro* studies have demonstrated that tau site-specific phosphorylation is correlated with a disease outcome[14-16]. Tau phosphorylation at Ser262 is an early taupathological event in AD, which is critical for Aβ-induced tau toxicity[17]. Accordingly, MAPK increases phospho-Ser262, which is the most prominently phosphorylated KXGS motif of tau[18]. The phosphorylation of Thr231 in AD is also marked as one of the earliest phosphorylated sites associated with regulating tau assembly, and inhibiting the ability of tau to stabilize microtubules in cells. Furthermore, the phosphorylation of Ser422 is increased in AD leading to increased tau filament formation.

Egb761 (Extract of *Ginkgo biloba* 761) is a potent antioxidant and free radical scavenger, which has anti-inflammatory[19], neuroprotective and platelet aggregator properties[20-22]. *Ginkgo biloba* extracts are commonly used as therapeutic agents in some cardiovascular disorders and a variety of neurological disturbances including Alzheimer's disease (AD)[23, 24]. In particular, Egb761 itself acts as an antioxidant and triggers the release of neuroprotectants to inhibit the neuropathological processes of AD including amyloid-β (Aβ)-induced neuronal death, Aβ oligomerization, and glial activation. Accordingly, Egb761 enhanced neurogenesis and prevented the occurrences of pathological behaviors

and cognitive impairments[24-26]. However, the neuroprotective effects of Egb761 on tau phosphorylation in neurons have not yet been reported.

Zinc is an important modulator of synaptic transmission and plasticity in the brain with the physiological concentration range of 10-20 μM. However, zinc levels are significantly increased in neuropathological conditions, e.g. AD, where zinc levels are increased in the hippocampus and cortex at concentrations of up to 300 μM [27-30]. Zinc plays multiple roles in the development/progression of AD, including a critical role in amyloid precursor protein processing and degradation of the Aβ peptide. An association between amyloid plaque accumulation and zinc has been reported and previous studies have suggested that zinc ions are involved in the development of AD[31-33]. Several recent studies have reported that zinc is also associated with tau phosphorylation, although the precise role of zinc in this process is unclear. Zinc treatment at high concentrations has shown to increase tau phosphorylation at a paired helical filament-1 site and to phosphorylate GSK3β at tyrosine 216 in human-tau-transfected cells[34]. In addition, zinc has shown to induce tau phosphorylation through the inhibition of Src-dependent protein phosphatase 2A (PP2A) inactivation. Therefore, zinc was used as a toxin to mimic AD in this study.

We aimed to investigate whether Egb761 inhibits tau phosphorylation in rat primary cortical neurons and the potential underlying mechanisms using zinc to model AD.

Materials and Methods

Materials

Pregnant Sprague-Dawley (SD) rats and male SD rats were obtained from Orient Bio Inc. (Seoul, Korea), and Fetal bovine serum (FBS), horse serum (HS), phosphate-buffered saline (PBS), and glutamine were purchased from Life Technologies Corporation (Grand Island, NY, USA). Minimum essential medium was purchased from JBI (Seoul, Korea). SB203580, SP600125, and U0126 were obtained from Merck KGaA (Darmstadt, Germany). LiCl, cytosine-β-arabinofuranoside, N-Acetyl-L-cysteine (NAC), poly D-lysine, D-glucose, and all other chemical reagents were purchased from Sigma-Aldrich Co. LLC (St. Louis, MO, USA). All experimental procedures were conducted using protocols approved by the Institutional Animal Care and Use Committee of Konkuk University (KU14163).

Source of *Ginkgo biloba* extract

Egb761 is a standardized *G. biloba* leaf extract that is used extensively in clinical trials. The extract contains 24% flavone glycosides (primarily composed of quercetin, kaempferol, and isorhamnetin) and 6% terpene lactones (2.8–3.4% ginkgolides A, B, and C, and 2.6–3.2% bilobalide). Other constituents include proanthocyanadins, glucose, rhamnose, organic acids (hydroxykynurenic, kynurenic, protocatechuic, vanillic, and shikimic acids), D-glucaric acid, ginkgolic acid (<5 ppm ginkgolic acids), and related alkylphenols. The Egb761 extracts were obtained from Dr. Willmar Schwabe, GmbH & Co. KG (Karlsruhe, Germany).

Cell culture

Primary cortical neuronal cultures were obtained by dissociation of the cortex of SD rats at embryonic day 18. The cortex was gently triturated mechanically three times with a flame-polished Pasteur pipette in culture medium (Eagle's minimal essential medium [MEM] supplemented with 20 mM glucose), and the dissociated cells were seeded onto 50 μg/mL poly-D-lysine-coated plates in culture medium supplemented with 5% fetal bovine serum, 5% HS, and 2 mM glutamine. The cultures were maintained at 37°C in a humidified 5% CO_2 incubator. For pure neuron cultures, 2 μM of cytosine-β-arabinofuranoside was added *in vitro* on the second day, as described in previous protocols [37]. Cultured neuronal cells were used on the eighth day *in vitro*. To examine the effects of Egb761 on zinc-induced toxicity in neurons, cells were exposed to various concentrations (50, 100, 200, 300, or 500 μM) of zinc chloride (Sigma-Aldrich Co. LLC) at various times periods (0.5, 1, 2, 3, 6, or 24 h) before being harvested for western blotting and cell viability measurements. Zinc was dissolved in PBS to make a 1 M stock solution, which was also diluted with PBS according to concentrations used in treatment. Egb761 was dissolved in methyl alcohol and was freshly diluted with PBS before use to produce a final Egb761-containing medium with 0.1% methyl alcohol concentration.

Western blot analysis

To investigate the effects of Egb761 on tau phosphorylation, cells were harvested and homogenized with 150 μl of RIPA (radioimmunoprecipitation assay) buffer containing 62.5 mM Tris-HCl (pH 6.8), 2% (w/v) sodium dodecyl sulfate (SDS), 10% glycerol, 10 mM 2-mercaptoethanol, 1 mM sodium orthovanadate, 100 μM phenylmethylsulfonyl fluoride, 1 μg/mL aprotinin, and 1 μg/mL leupeptin per well. Samples were centrifuged for 30 min at 4°C and the protein content of each sample was measured by a bicinchoninic acid protein (BCA) assay. Equal amounts of protein from each sample (10 μg/mL) were transferred into new tubes and boiled for 5 min. Protein samples were separated by 10% SDS-polyacrylamide gel electrophoresis for 120 min and were electrophoretically transferred onto nitrocellulose membranes (GE Healthcare Bio-Sciences, Pittsburgh, PA, USA) for 90 min. The

blots were blocked with 5% nonfat dried milk at room temperature and incubated overnight at 4°C with anti-phospho-tau Ser262 (1:2000; Life Technologies Corporation), anti-phospho-tau Thr231 (1:2000; Life Technologies Corporation), anti-phospho-tau Ser199 (1:1000; Life Technologies Corporation), anti-phospho-tau Ser396 (1:1000; Cell Signaling Technology, Inc., Danvers, MA, USA), anti-tau (1:2000; Life Technologies Corporation), anti-phospho-extracellular-signal regulated kinase 1/2 (ERK1/2) Thr202/Tyr204 (1:2000; Cell Signaling Technology, Inc.), anti-ERK1/2 (1:2000; Cell Signaling Technology, Inc.), anti-phospho-p38 Thr180/Tyr182 (1:1000; Cell Signaling Technology, Inc.), anti-p38 (1:1000; Cell Signaling Technology, Inc.), anti-phospho-c-Jun N-terminal kinase (JNK) Thr183/Tyr185 (1:1000, Cell Signaling Technology, Inc.), anti-JNK (1:1000; Cell Signaling Technology, Inc.), anti-phospho-GSK3β Ser9 (1:2000; Cell Signaling Technology, Inc.), anti-phospho-GSK3β Tyr279/Tyr216 (1:1000, EMD Millipore Corporation, Billerica, MA, USA), and anti-GSK3β (1:2000; Cell Signaling Technology, Inc.) primary antibodies diluted in 5% nonfat dried milk IN TBST solution. Membranes were washed three times with 0.01% Tween-20 in Tris-buffered saline and incubated with appropriate horseradish peroxidase-conjugated secondary antibodies at room temperature for 2 h. The bands were detected with an enhanced chemiluminescence system (Intron Bio. Korea). Bands were exposed on a LAS-3000 image detection system (Fuji Corporation, Tokyo, Japan) by ECL and quantified by Image J. Signal density was normalized to β-actin levels (Sigma-Aldrich Co. LLC) measured by western blot analyses at a dilution of 1:30000.

Measurement of Cell viability

The effects of Egb761 on zinc-induced neuronal death were investigated using a 3-[4,5-dimethylthiazol-2-yl]-2,5-diphenyl-tetrazolium bromide (MTT) assay. MTT is a water-soluble tetrazolium salt that is reduced to a colored and water-insoluble formazan salt by metabolically viable cells. MTT (2 mg/mL) was added to the cell-culture medium and incubated at 37°C for 2 h in a 5% CO_2 atmosphere. The MTT reaction was suspended by replacing the MTT-containing medium with dimethylsulfoxide, and the absorbance was read at 570 nm with a microplate reader (Molecular Devices, LLC, Sunnyvale, CA, USA). The percentage of neuronal survival was derived by considering the absorbance of vehicle-treated cells as 100% [37].

Measurement of intracellular levels of ROS

Intracellular ROS formation was measured through fluorescence with 2',7'-dichlorodihydrofluorescein diacetate ($DCFH_2$-DA; Life Technologies Corporation). After drug treatment, the cultures were washed with Hank's balanced aqueous salts solution containing 120 mM NaCl, 5 mM KCl, 1.6 mM $MgCl_2$, 2.3 mM $CaCl_2$, 15 mM glucose, 20 mM HEPES, and 10 mM NaOH and loaded with 20 μM

of $DCFH_2$-DA for 30 min at 37°C. $DCFH_2$-DA fluorescence was analyzed with a fluorescence plate reader (Spectramax Gemini EM, Life Technologies Corporation) at an excitation of 490 nm and an emission of 530 nm that was detected with a fluorescent microscope.

Immunocytochemistry

Zinc-treated cells were fixed with ice-cold 4% paraformaldehyde in PBS (pH 7.4) for 20 min. Fixed cells were washed with PBS and were added with blocking buffer (10% HS and 0.3% Triton X-100 in PBS) for 1 h at room temperature. Cells were incubated overnight at 4°C in primary antibodies against neurons (NeuN, 1: 1,000) and phospho-tau at Ser262 (1:500) and rinsed with washing buffer (1.5% HS and 0.1 % Triton X-100 in PBS) three times. Then, cells were incubated with appropriate secondary antibodies conjugated to either Alexa488 or Alexa594, diluted in blocking buffer, for 2 h at room temperature. Cells were washed three times with washing buffer, mounted with Prolong gold (Life Technologies Corporation) and visualized with a confocal microscope (LSM 710, Carl Zeiss Microscopy Co., Ltd., Tokyo, Japan).

Statistical analysis

All results were quantified and expressed as means ± the standard error of the mean (SEM). Statistical comparisons were performed through one-way ANOVA followed by Tukey's *posthoc* test using the SPSS software (IBM Corporation, Armonk, NY, USA). Results were considered significant when p values were less than 0.05.

Results

Zinc induced tau phosphorylation at Ser262 and neuronal cell death with intracellular reactive oxygen species in rat primary cortical neurons

To investigate the effects of zinc on tau phosphorylation in rat primary cortical neurons, the levels of tau phosphorylation at four sites (Ser262, Ser396, Thr231, and Ser199) were examined. Rat primary cortical neurons were incubated in serum-free MEM containing 300 μM zinc for various durations at 37°C. Zinc treatment began to increase tau phosphorylation at Ser262 from 30 min and showed maximal increase at 3 h. Cultured neurons were treated with different concentrations (0, 50, 100, 200, 300, or 500 μM) of zinc for 2 h at 37°C. Zinc-induced tau phosphorylation at Ser262 was markedly enhanced in a concentration-dependent manner compared to the control (Fig. 1). Tau phosphorylation by zinc at other sites, such as Ser396, Thr231, and Ser199, did not change (Supplementary Fig.1). In

addition, zinc increased neuronal cell death upon 3 h incubation, and 300 μM zinc significantly increased intracellular ROS levels at 30 min (Fig. 2). These results indicate that high amount of zinc induced tau phosphorylation at Ser262 in rat primary cortical neurons along with increased intracellular ROS levels. Based on these results, rat primary cortical neurons were treated with zinc at a dose of 300μM for 2 h for the following experiments as these conditions showed the maximal AD-mimicking effect of zinc.

Egb761 attenuated zinc-induced tau hyperphosphorylation

To investigate the effects of Egb761 on zinc-induced tau phosphorylation, cells were pretreated with 50–500 μM of Egb761 for 1 h, followed by treatment with 300 μM zinc for 2 h. Levels of tau phosphorylation at Ser262 were measured by western blot analyses. Zinc-induced tau phosphorylation was significantly reduced by Egb761 treatment (Fig. 3A). Immunostaining of primary cortical neurons also showed the inhibiting effects of Egb761 on zinc-induced tau phosphorylation (Fig. 3C). To further examine the effects of Egb761 on zinc-induced tau phosphorylation, rat hippocampal organotypic slice cultures were analyzed (Fig. 3B). Confirmatively, zinc induced tau hyperphosphorylation at Ser262, which was prevented by Egb761 treatment (Fig. 3). These data demonstrate the potential of Egb761 to counteract zinc-induced tau phosphorylation at Ser262 in rat primary cortical neurons and hippocampal slice cultures.

Egb761 regulated the tau protein kinases, including GSK3β

To identify the tau kinases associated with tau phosphorylation, we examined the expression levels of the tau kinases, GSK3β, MAPKs, and CDK5, with Western blot analyses. The cultured neurons were treated with zinc, and the total protein was extracted at different time periods (15 min, 30 min, 1 h, 2 h, and 3 h). Cells were treated with various concentration of zinc, and the total protein extracts were assayed after 2 h. Zinc activated phospho-ERK1/2, phospho-p38, and phospho-GSK3β (Ser9) in a time- and concentration-dependent manner (Fig. 4). Furthermore, the effects of the inhibitors of tau kinases on tau phosphorylation at Ser262 were examined. Zinc-induced tau phosphorylation was reduced by SB203080 (a specific inhibitor of p38 MAPK, 20 μM), SP600125 (a specific inhibitor of JNK, 10 μM), and Lithium Chloride (LiCl) (a specific inhibitor of GSK3β, 10 mM). These data indicated that zinc-induced tau phosphorylation was mediated by GSK3β (Fig. 5). Next, the effects of Egb761 on the phosphorylation of GSK3β were examined. Indeed, Egb761 inhibited the phosphorylation of GSK3β (Ser9) (Fig. 6). In addition, Egb761 inhibited the zinc-induced neuronal cell death and decreased the intracellular ROS levels. LiCl attenuated zinc-induced cell death, but not intracellular ROS levels at least within this time range. To clarify whether the increased intracellular

ROS levels were mediated by zinc-induced tau phosphorylation, cells were preincubated with N-acetylcysteine (NAC; 1 mM, 1 h), followed by 300 μM zinc treatment for an additional 2 h, and the levels of tau phosphorylation at Ser262 were measured. The results demonstrate that NAC attenuated the zinc-induced tau phosphorylation, indicating that the increased intracellular ROS levels were dependent on zinc-induced tau phosphorylation (Fig. 5). These data showed that zinc strongly activated the GSK3β tau kinase and that Egb761 inhibited the GSK3β (Ser9) phosphorylation in both ROS-dependent and -independent manner.

Discussion

In the brain, excessive amount of zinc promotes amyloid plaque aggregation and tau hyperphosphorylation, resulting in neuronal cell death [38]. Zinc levels are increased in the brain regions that are severely affected in AD [39]. In this study, we found that Egb761 inhibits tau phosphorylation at Ser262 of rat primary cortical neurons induced by high zinc, through GSK3β and ROS-related mechanisms, demonstrating the neuroprotective property of Egb761.

Tau phosphorylation may result from an imbalance between tau kinases such p38 MAPK, and tau phosphatases such as PP2A. Various serine/threonine and tyrosine residues on tau are phosphorylated by CDK5, calcium/calmodulin-dependent protein kinase II, MAPK, and GSK3β; whereas dephosphorylated by PP2A. The present study showed that zinc regulated tau phosphorylation at Ser262 through GSK3β but not by CDK5, calcium/calmodulin-dependent protein kinase II or PP2A in rat primary cortical neurons. It has been previously reported that zinc does not alter PP2A activity in SH-SY5Y cells [40] but induces PP2A inactivation through src tyrosine kinase in brains with AD [30]. Our data showed that the phosphorylation of GSK3β at Tyr216/279 and Ser9 was increased by zinc although we did not examine the expression of src tyrosine kinase. Further study of these issues will be required to elucidate the mechanisms by which zinc modulated tau phosphorylation.

GSK3β is a tau kinase that has been linked to both the sporadic and genetic forms of AD. GSK, is composed of GSK3β and GSK3α and is well known as a master kinase that regulates a variety of cellular functions by serine/threonine phosphorylation. The inhibition of GSK3 activity has been studied as a novel therapeutic approach for AD [41, 42]. Between the two isotypes of GSK, most AD-related studies have concentrated on GSK3β rather than GSK3α. It was found that GSK-3 increases Aβ production by regulating amyloid precursor protein cleavage [43, 44] and tau phosphorylation [45, 46]. Accordingly, lithium is known to inhibit GSK3 both directly and indirectly. Thus, GSK3 inhibition by lithium treatment could possibly reverse AD pathology through reduction of Aβ levels [44, 46]. In

addition, a previous study showed that lithium treatment inhibits tau phosphorylation at Ser262 [47]. Herein, we showed that GSK3β inhibition by lithium treatment prevented tau phosphorylation at Ser262, whereas NAC showed similar effects. However, lithium did not inhibit intracellular ROS levels. We thus suggest that zinc induction of rat primary cortical neurons increased the intracellular ROS levels leading to the activation of GSK3 and tau phosphorylation.

Egb761, the standardized *Ginkgo biloba* extract, is well-known potent antioxidant[48,49]. It has been reported that Egb761 prevents Aβ-induced neurotoxicity by inhibiting the intracellular ROS accumulation[50,51]. Moreover, in aging rat brains, EGb761 provides the neuroprotective effects through GSH and SOD recovery against acute hyoxia[52] and age-associated with oxidative damage to mitochondria[53]. The cellular effects of Egb761 are associated with modulation of intracellular signaling cascades such as phosphorylation of cyclic AMP response element-binding protein (CREB), Akt, ERK1/2 and JNK[48,49]. A previous study showed zinc increased tau S214 phosphorylation by the activation of MEK1/2 in tau-expressing SH-SY5Y cells[54]. These data indicate protective effects of Egb761 could be associated with inhibition of the signaling pathways such as ERK1/2 and JNK activated by zinc.

There are many sites of tau phosphorylation including Ser262, Ser356, and Thr231. Nevertheless, our data showed that zinc increased tau phosphorylation only at Ser262 in rat primary cortical neurons. A previous study had shown that zinc induces tau phosphorylation at Ser262/356 in SH-SY5Y cells [40]. Tau phosphorylation at Ser262 in pretangle neurons is an early event in tauopathy [36]. Human Aβ42 increases tau phosphorylation at Ser262 and promotes tau-induced neuronal death [17]. Although the precise pathophysiology is not fully known, it is increasingly evident that tau phosphorylation at Ser262 may be an important therapeutic target for neurodegenerative diseases such as AD.

Conclusions

Our results indicate a possible role of Egb761 in the regulation of tau phosphorylation which involves the following mechanisms: 1) direct inhibition of intracellular ROS, 2) direct inhibition of GSK3β phosphorylation, and 3) inhibition of GSK3β through ROS downregulation (Fig. 7). These findings suggest that Egb761 may be a candidate compound to inhibit tau hyperphosphorylation, a characteristic feature of AD and other tauopathies. Furthermore, the regulation of zinc homeostasis could be a promising therapeutic target for AD and related tauopathies.

Acknowledgement

This work was supported by Basic Science Research Program through the National Research Foundation of Korea (NRF) funded by the Ministry of Education to Kyoung Ja Kwon (NRF-2010-0023638) and by the Ministry of Science, ICT & Future Planning (2013R1A1A2074860) to Seol-Heui Han.

Disclosure

The authors declare no conflict of interest.

References

1. K. S. Kosik, C. L. Joachim and D. J. Selkoe, *Proceedings of the National Academy of Sciences of the United States of America*, 1986, **83**, 4044-4048.
2. I. Grundke-Iqbal, K. Iqbal, M. Quinlan, Y. C. Tung, M. S. Zaidi and H. M. Wisniewski, *The Journal of biological chemistry*, 1986, **261**, 6084-6089.
3. D. P. Hanger, B. H. Anderton and W. Noble, *Trends in molecular medicine*, 2009, **15**, 112-119.
4. J. Bertrand, V. Plouffe, P. Senechal and N. Leclerc, *Neuroscience*, 2010, **168**, 323-334.
5. G. V. Johnson and W. H. Stoothoff, *Journal of cell science*, 2004, **117**, 5721-5729.
6. M. Goedert, *Current opinion in genetics & development*, 2001, **11**, 343-351.
7. D. H. Cho, E. J. Lee, K. J. Kwon, C. Y. Shin, K. H. Song, J. H. Park, I. Jo and S. H. Han, *Journal of neurochemistry*, 2013, **126**, 685-695.
8. S. Jayapalan and J. Natarajan, *Bioinformation*, 2013, **9**, 1023-1030.
9. M. Cao, F. Liu, F. Ji, J. Liang, L. Liu, Q. Wu and T. Wang, *Behavioural brain research*, 2013, **237**, 249-255.
10. G. Drewes, B. Lichtenberg-Kraag, F. Doring, E. M. Mandelkow, J. Biernat, J. Goris, M. Doree and E. Mandelkow, *The EMBO journal*, 1992, **11**, 2131-2138.
11. C. H. Reynolds, A. R. Nebreda, G. M. Gibb, M. A. Utton and B. H. Anderton, *Journal of neurochemistry*, 1997, **69**, 191-198.
12. C. Feijoo, D. G. Campbell, R. Jakes, M. Goedert and A. Cuenda, *Journal of cell science*, 2005, **118**, 397-408.
13. M. Goedert, M. Hasegawa, R. Jakes, S. Lawler, A. Cuenda and P. Cohen, *FEBS letters*, 1997, **409**, 57-62.
14. A. C. Alonso, I. Grundke-Iqbal and K. Iqbal, *Nature medicine*, 1996, **2**, 783-787.
15. L. Buee, T. Bussiere, V. Buee-Scherrer, A. Delacourte and P. R. Hof, *Brain research. Brain research reviews*, 2000, **33**, 95-130.
16. J. H. Cho and G. V. Johnson, *The Journal of biological chemistry*, 2003, **278**, 187-193.

17. K. Iijima, A. Gatt and K. Iijima-Ando, *Human molecular genetics*, 2010, **19**, 2947-2957.
18. M. A. Jensen, T. R. Koszalka and R. L. Brent, *Developmental biology*, 1975, **42**, 1-12.
19. Y. Oyama, L. Chikahisa, T. Ueha, K. Kanemaru and K. Noda, *Brain research*, 1996, **712**, 349-352.
20. E. J. Lee, H. Y. Chen, T. S. Wu, T. Y. Chen, I. A. Ayoub and K. I. Maynard, *Journal of neuroscience research*, 2002, **68**, 636-645.
21. S. Saleem, H. Zhuang, S. Biswal, Y. Christen and S. Dore, *Stroke; a journal of cerebral circulation*, 2008, **39**, 3389-3396.
22. P. F. Smith, K. Maclennan and C. L. Darlington, *Journal of ethnopharmacology*, 1996, **50**, 131-139.
23. C. M. Watanabe, S. Wolffram, P. Ader, G. Rimbach, L. Packer, J. J. Maguire, P. G. Schultz and K. Gohil, *Proceedings of the National Academy of Sciences of the United States of America*, 2001, **98**, 6577-6580.
24. F. V. DeFeudis and K. Drieu, *Current drug targets*, 2000, **1**, 25-58.
25. Y. Luo, J. V. Smith, V. Paramasivam, A. Burdick, K. J. Curry, J. P. Buford, I. Khan, W. J. Netzer, H. Xu and P. Butko, *Proceedings of the National Academy of Sciences of the United States of America*, 2002, **99**, 12197-12202.
26. F. Tchantchou, Y. Xu, Y. Wu, Y. Christen and Y. Luo, *FASEB journal : official publication of the Federation of American Societies for Experimental Biology*, 2007, **21**, 2400-2408.
27. M. A. Deibel, W. D. Ehmann and W. R. Markesbery, *Journal of the neurological sciences*, 1996, **143**, 137-142.
28. D. Religa, D. Strozyk, R. A. Cherny, I. Volitakis, V. Haroutunian, B. Winblad, J. Naslund and A. I. Bush, *Neurology*, 2006, **67**, 69-75.
29. A. S. Nakashima, S. Oddo, F. M. Laferla and R. H. Dyck, *Neurobiology of aging*, 2010, **31**, 605-613.
30. Y. Xiong, X. P. Jing, X. W. Zhou, X. L. Wang, Y. Yang, X. Y. Sun, M. Qiu, F. Y. Cao, Y. M. Lu, R. Liu and J. Z. Wang, *Neurobiology of aging*, 2013, **34**, 745-756.
31. A. I. Bush, W. H. Pettingell, G. Multhaup, M. d Paradis, J. P. Vonsattel, J. F. Gusella, K. Beyreuther, C. L. Masters and R. E. Tanzi, *Science*, 1994, **265**, 1464-1467.
32. W. P. Esler, E. R. Stimson, J. M. Jennings, J. R. Ghilardi, P. W. Mantyh and J. E. Maggio, *Journal of neurochemistry*, 1996, **66**, 723-732.
33. R. A. Cherny, C. S. Atwood, M. E. Xilinas, D. N. Gray, W. D. Jones, C. A. McLean, K. J. Barnham, I. Volitakis, F. W. Fraser, Y. Kim, X. Huang, L. E. Goldstein, R. D. Moir, J. T. Lim, K. Beyreuther, H. Zheng, R. E. Tanzi, C. L. Masters and A. I. Bush, *Neuron*, 2001, **30**, 665-676.
34. A. Boom, M. Authelet, R. Dedecker, C. Frederick, R. Van Heurck, V. Daubie, K. Leroy, R. Pochet and J. P. Brion, *Biochimica et biophysica acta*, 2009, **1793**, 1058-1067.
35. J. E. Jan, R. J. Reiter, M. C. Bax, U. Ribary, R. D. Freeman and M. B. Wasdell, *European journal of paediatric neurology : EJPN : official journal of the European Paediatric Neurology Society*, 2010, **14**, 380-390.
36. J. C. Augustinack, A. Schneider, E. M. Mandelkow and B. T. Hyman, *Acta neuropathologica*, 2002, **103**, 26-35.

37. K. J. Kwon, J. N. Kim, M. K. Kim, J. Lee, L. J. Ignarro, H. J. Kim, C. Y. Shin and S. H. Han, *Journal of pineal research*, 2011, **50**, 110-123.
38. J. Gotz, F. Chen, J. van Dorpe and R. M. Nitsch, *Science*, 2001, **293**, 1491-1495.
39. G. Danscher, K. B. Jensen, C. J. Frederickson, K. Kemp, A. Andreasen, S. Juhl, M. Stoltenberg and R. Ravid, *Journal of neuroscience methods*, 1997, **76**, 53-59.
40. F. Zhou, S. Chen, J. Xiong, Y. Li and L. Qu, *Biological trace element research*, 2012, **149**, 273-279.
41. M. K. King, M. Pardo, Y. Cheng, K. Downey, R. S. Jope and E. Beurel, *Pharmacology & therapeutics*, 2014, **141**, 1-12.
42. F. Yu, Y. Zhang and D. M. Chuang, *Journal of neurotrauma*, 2012, **29**, 2342-2351.
43. C. Hooper, R. Killick and S. Lovestone, *Journal of neurochemistry*, 2008, **104**, 1433-1439.
44. E. Rockenstein, M. Torrance, A. Adame, M. Mante, P. Bar-on, J. B. Rose, L. Crews and E. Masliah, *The Journal of neuroscience : the official journal of the Society for Neuroscience*, 2007, **27**, 1981-1991.
45. H. Park, T. I. Kam, Y. Kim, H. Choi, Y. Gwon, C. Kim, J. Y. Koh and Y. K. Jung, *Human molecular genetics*, 2012, **21**, 2725-2737.
46. J. J. Lucas, F. Hernandez, P. Gomez-Ramos, M. A. Moran, R. Hen and J. Avila, *The EMBO journal*, 2001, **20**, 27-39.
47. Y. J. Zhang, Y. F. Xu, Y. H. Liu, J. Yin and J. Z. Wang, *FEBS letters*, 2005, **579**, 6230-6236.
48. C. Shi, L. Zhao, B. Zhu, Q. Li, D. T. Yew, Z. Yao and J. Xu, *Chemico-biological interactions*, 2009, **181**, 115-123.
49. C. Shi, L. Zhao, B. Zhu, Q. Li, D. T. Yew, Z. Yao and J. Xu, *Chemico-biological interactions*, 2009, **180**, 389-397.
50. S. Bastianetto, C. Ramassamy, S. Dore, Y. Christen, J. Poirier and R. Quirion, *The European journal of neuroscience*, 2000, **12**, 1882-1890.
51. J. V. Smith and Y. Luo, *Journal of Alzheimer's disease : JAD*, 2003, **5**, 287-300.
52. R. Martin, C. Mozet, H. Martin, K. Welt, C. Engel and G. Fitzl, *Aging clinical and experimental research*, 2011, **23**, 255-263.
53. J. Sastre, A. Millan, J. Garcia de la Asuncion, R. Pla, G. Juan, Pallardo, E. O'Connor, J. A. Martin, M. T. Droy-Lefaix and J. Vina, *Free radical biology & medicine*, 1998, **24**, 298-304.
54. I. Kim, E. J. Park, J. Seo, S. J. Ko, J. Lee and C. H. Kim, *Neuroreport*, 2011, **22**, 839-844.

Figure legends

Figure 1. Zinc induces tau phosphorylation at Ser262 in rat primary cortical neurons. A. Time-dependent effect of 300 μM $ZnCl_2$ treatment. Rat primary cortical neurons were incubated in serum-free MEM with 300 μM $ZnCl_2$ for varying durations (0.5, 1, 2, 3, or 6 h). B. Dose-dependent effect of $ZnCl_2$ treatment. Cultured cells were treated with increasing concentrations of $ZnCl_2$ (50, 100, 200, 300, or 500 μM) for 3 h at 37°C. The cells were harvested for Western blot analyses, and the expression of tau phosphorylation was assessed by measuring levels of immunoreactivity to the phospho-tau Ser262 antibody. Total amounts of tau and β-actin were measured and used as controls. The data represent the mean ± S.E.M. (n = 4). * $p < 0.05$, ** $p < 0.01$ CON vs. $ZnCl_2$.

Figure 2. Zinc induces cell death and ROS generation in rat primary cortical neurons. A. Rat primary cortical neurons were incubated in serum-free MEM with various concentrations of $ZnCl_2$ (50, 100, 200, 300, or 500 μM) for 3 h at 37°C. Cell viability was measured through MTT assay. B. Rat primary cortical neurons were incubated in serum-free MEM with 300 μM $ZnCl_2$ and in varying durations (0.5, 1, 2, 3, or 6 h) at 37°C. Intracellular ROS was measured by $DCFH_2$-DA fluorescence (490/530 nm). The data represent the mean ± S.E.M. (n = 4). * $p < 0.05$, ** $p < 0.01$ CON vs. $ZnCl_2$.

Figure 3. Egb761 prevents zinc-induced tau phosphorylation at Ser 262. A. Effects of Egb761 on zinc-induced tau phosphorylation in rat cortical neurons. Rat primary cortical neurons were pretreated with Egb761 (50, 100, 200, or 500 μg/mL) for 1 h and incubated with 300 μM $ZnCl_2$ for 2 h in serum-free MEM. Cells were harvested for Western blot analyses, and the expression of tau phosphorylation was assessed by measuring the levels of immunoreactivity to the phospho-Tau-Ser262 antibody. Total amounts of tau and β-actin were measured and used as controls. The graph shows the densitometric quantification data of the phospho-Tau-Ser262 band intensities. The data represents the mean ± S.E.M. (n = 2). * $p < 0.05$, ** $p < 0.01$ CON vs. $ZnCl_2$, # $p < 0.05$, ## $p < 0.01$ $ZnCl_2$ vs. Egb761. B. Effects of Egb761 on zinc-induced tau phosphorylation at Ser262 in rat organotypic hippocampal slice cultures. Rat slice cultures were pretreated with Egb761 for 1 h and then incubated with 300 μM $ZnCl_2$ for 2 h in Eagle's basal medium. C. Immunostaining of tau phosphorylation at Ser262 in rat primary cortical neurons. Cells were pretreated with Egb761 (200 μg/mL) for 1 h and then incubated with 300 μM of $ZnCl_2$ for 2 h in serum-free MEM. Treated cells were fixed and the expression of tau phosphorylation was assessed by measuring the levels of immunoreactivity to the phospho-Tau-Ser262 antibody with immunocytochemistry. Bar size = 20 μm.

Figure 4. Zinc-induced signaling pathways that phosphorylate tau in rat primary cortical neurons. Rat primary cortical neurons were incubated in serum-free MEM with 500 μM $ZnCl_2$ and in varying durations (15 min–3 h) with increasing concentrations of $ZnCl_2$ (50, 100, 200, 300, or 500 μM) for 3 h at 37°C. A. B. Cells were harvested for western blot analyses, and the activation of ERK, p38, JNK, and GSK3β were assessed by measuring each of the respective phosphorylated forms of these signaling proteins. The total amounts of ERK, p38, JNK, and GSK3β were measured and used as controls. The data represent the mean ± S.E.M. (n = 4). * $p < 0.05$, ** $p < 0.01$ CON vs. $ZnCl_2$.

Figure 5. The association of GSK3β activation with tau phosphorylation. Rat primary cortical neurons were pretreated with inhibitors (10 μM SP600125, 20 μM SB203580, 10 μM U0126, 10 mM LiCl, or 1 mM N-acetylcysteine) for 1 h and then incubated with 300 μM of $ZnCl_2$ for 2 h in serum-free MEM (A,B). A. Cells were harvested for Western blot analyses, and the levels of tau phosphorylation were assessed by measuring levels of immunoreactivity to the phospho-Tau Ser262 antibody. Total amounts of tau and β-actin were measured and used as controls. B. The graph shows the densitometric quantification data of the phospho-Tau Ser262 band intensities. Rat primary cortical neurons were pretreated with Egb761 and MAPK inhibitors for 1 h and then incubated with 300 μM $ZnCl_2$ for 2 h in serum-free MEM (C,D). C. Cell viability was measured through MTT assay. The data represent the mean ± S.E.M. (n = 4). * $p < 0.05$, ** $p < 0.01$, # $p < 0.05$, ## $p < 0.01$. D. Intracellular ROS levels were measured with H_2DCF-DA fluorescence (490/530 nm). The data represent the mean ± S.E.M. (n = 4). * $p < 0.05$, ** $p < 0.01$ CON vs. $ZnCl_2$, # $p < 0.05$, ## $p < 0.01$ $ZnCl_2$ vs. inhibitors. The data represent the mean ± S.E.M. (n = 6). * $p < 0.05$, ** $p < 0.01$ CON vs. $ZnCl_2$, # $p < 0.05$, ## $p < 0.01$ $ZnCl_2$ vs. inhibitors.

Figure 6. The effects of Egb761 on GSK3β activation in primary cortical neurons. Rat primary cortical neurons were pretreated with Egb761 (50-500 μg/mL) for 1 h and then incubated with 300 μM $ZnCl_2$ for 2 h in serum-free MEM. A**.** Cells were harvested for western blot analyses, and the expression of GSK3β was assessed by measuring the phospho-GSK3β-Ser9 antibody. Total amounts of GSK3β and β-actin were measured and used as controls. B. The graph shows the densitometric quantification data of the phospho-GSK3β-Ser9 band intensities. The data represent the mean ±S.E.M. (n=6) *$p < 0.05$, ** $p < 0.01$, # $p < 0.05$, ## $p < 0.01$.

Figure 7. Diagrammatic scheme illustrating the effects of Egb761 in rat primary cortical neurons. Egb761 inhibits tau phosphorylation at Ser262 through 3 pathways: 1. the direct inhibition of intracellular ROS, 2. the direct inhibition of GSK3β phosphorylation, and 3. the inhibition of GSK3β through ROS downregulation.

Graphic abstract

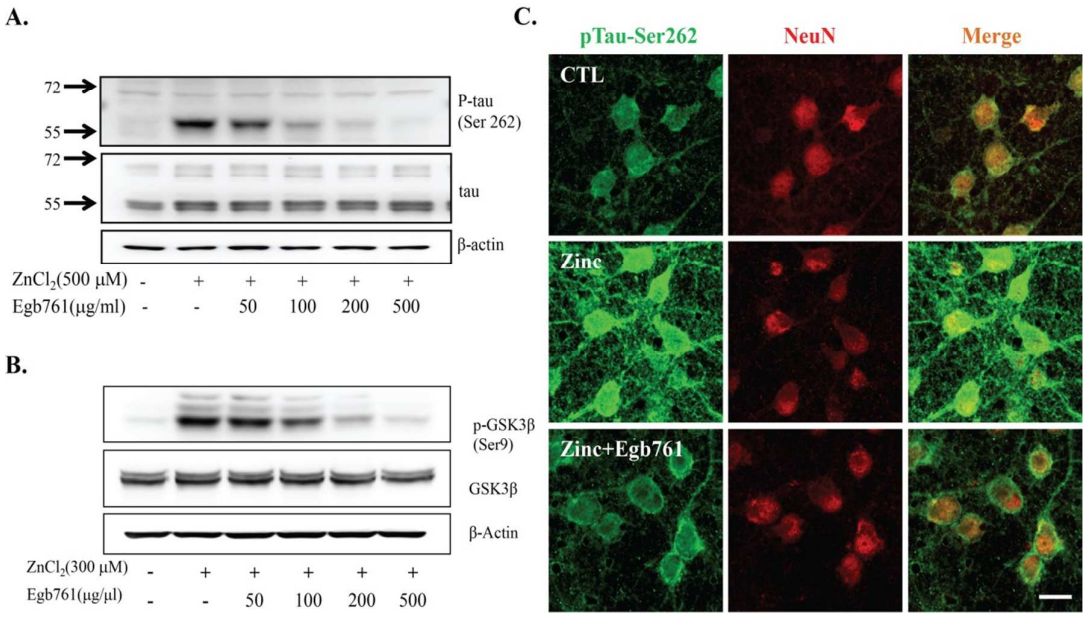

- Egb761 attenuates zinc-induced tau hyperphosphorylation at Ser262.
- Egb761 inhibites GSK3beta (Ser9) phosphorylation ROS-dependently and -independently.
- Egb761 may be effective in the treatment of tauopathy in neurological disorders, such as Alzheimer's disease.

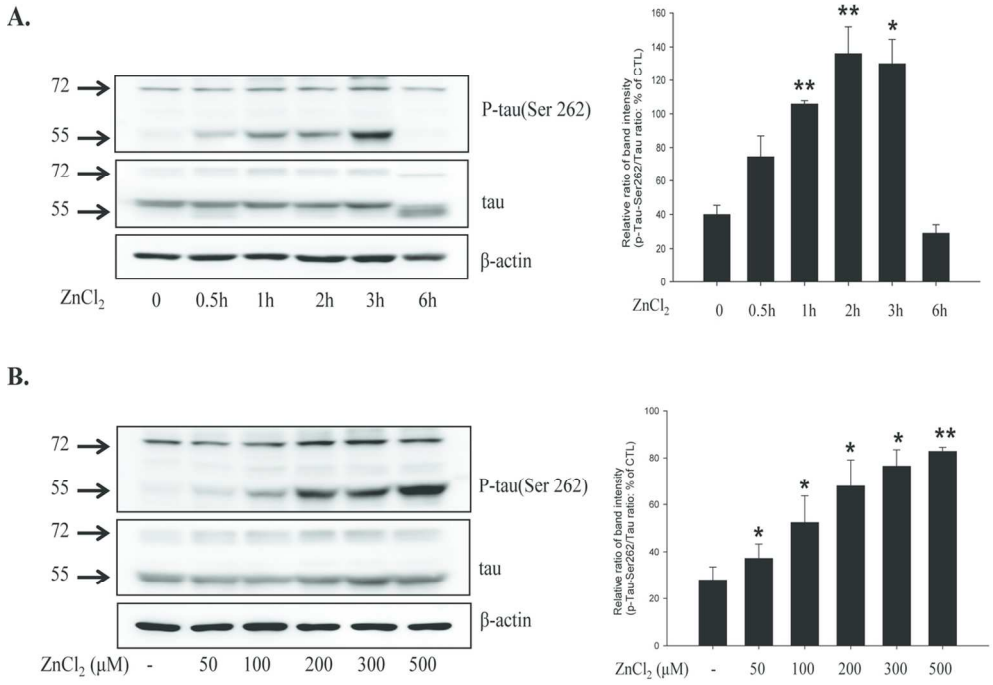

Figure 1. Zinc induces tau phosphorylation at Ser262 in rat primary cortical neurons. A. Time dependency of 300 μM $ZnCl_2$. Rat primary cortical neurons were incubated in serum-free MEM with 300 μM $ZnCl_2$ for varying durations (0.5, 1, 2, 3, or 6 h). B. Dose dependency of $ZnCl_2$. Cultured cells were treated with increasing concentrations of $ZnCl_2$ (50, 100, 200, 300, or 500 μM) for 3 h at 37°C. The cells were harvested for Western blot analyses, and the expression of tau phosphorylation was assessed by measuring levels of immunoreactivity to the phospho-tau Ser262 antibody. Total amounts of tau and β-actin were measured and used as controls. The data represent the mean ± standard error of the mean (S.E.M.; n = 4). * $p < 0.05$, ** $p < 0.01$ CON vs. $ZnCl_2$.
116x82mm (300 x 300 DPI)

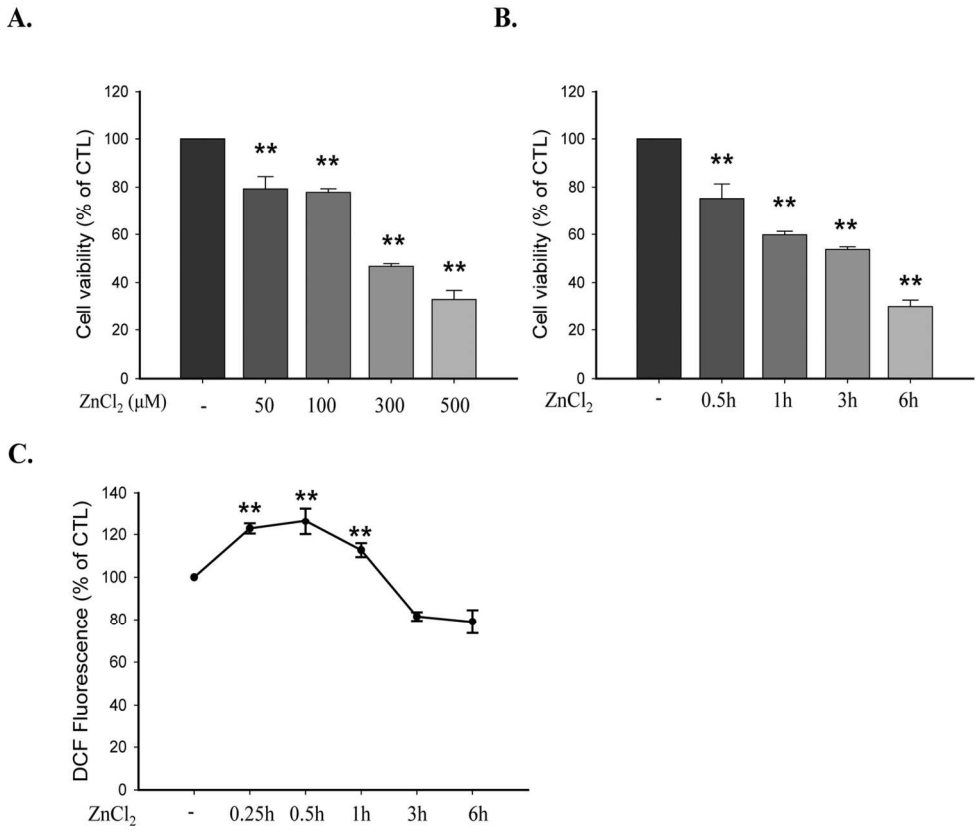

Figure 2. Zinc induces cell death and ROS generation in rat primary cortical neurons. A. Rat primary cortical neurons were incubated in serum-free MEM with various concentrations of $ZnCl_2$ (50, 100, 200, 300, or 500 μM) for 3 h at 37°C. Cell viability was measured with a MTT assay. B. Rat primary cortical neurons were incubated in serum-free MEM with 300 μM $ZnCl_2$ for varying durations (0.5, 1, 2, 3, or 6 h) at 37°C. Intracellular ROS was measured by $DCFH_2$-DA fluorescence (490/530 nm). The data represent the mean ± S.E.M. (n = 4). * $p < 0.05$, ** $p < 0.01$ CON vs. $ZnCl_2$.
129x107mm (300 x 300 DPI)

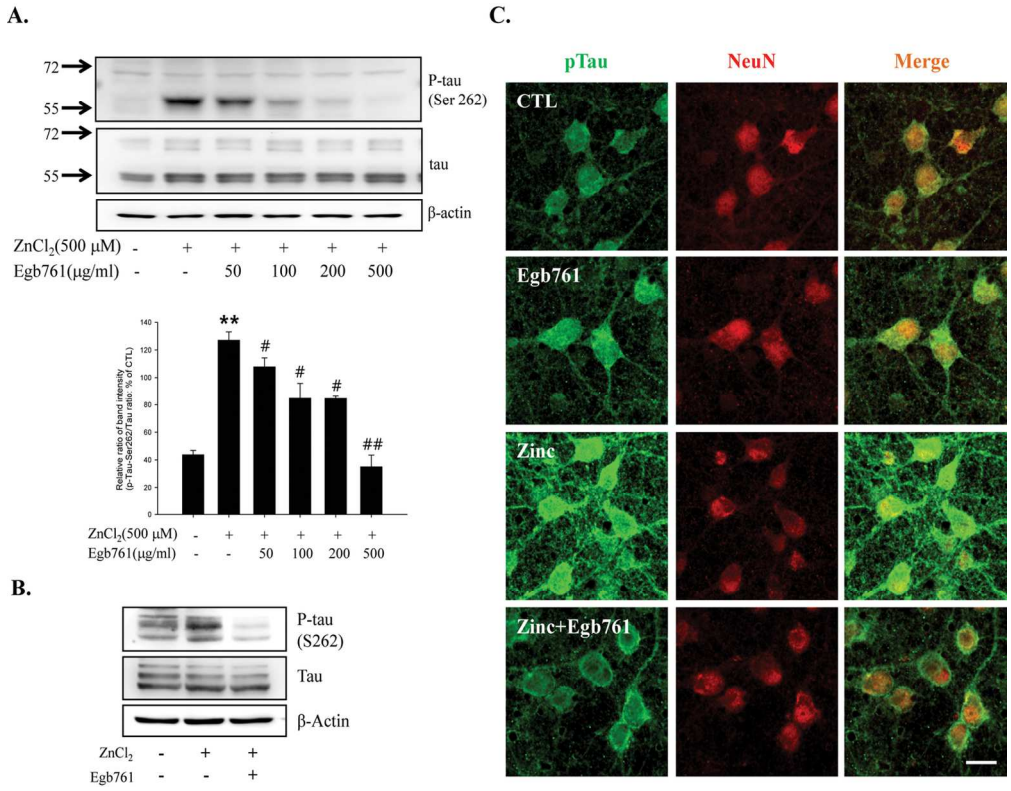

Figure 3. Egb761 prevents zinc-induced tau phosphorylation at Ser 262. A. Effects of Egb761 on zinc-induced tau phosphorylation in rat cortical neurons. Rat primary cortical neurons were pretreated with Egb761 (50, 100, 200, or 500 μg/mL) for 1 h and incubated with 300 μM $ZnCl_2$ for 2 h in serum-free MEM. Cells were harvested for Western blot analyses, and the expression of tau phosphorylation was assessed by measuring the levels of immunoreactivity to the phospho-Tau-Ser262 antibody. Total amounts of tau and β-actin were measured and used as controls. The graph shows the densitometric quantification data of the phospho-Tau-Ser262 band intensities. The data represents the mean ± S.E.M. (n = 2). * $p < 0.05$, ** $p < 0.01$ CON vs. $ZnCl_2$, $^{\#}$ $p < 0.05$, $^{\#\#}$ $p < 0.01$ $ZnCl_2$ vs. Egb761. B. Effects of Egb761 on zinc-induced tau phosphorylation at Ser262 in rat organotypic hippocampal slice cultures. Rat slice cultures were pretreated with Egb761 for 1 h and then incubated with 300 μM $ZnCl_2$ for 2 h in Eagle's basal medium. C. Immunostaining of tau phosphorylation at Ser262 in rat primary cortical neurons. Cells were pretreated with Egb761 (200 μg/mL) for 1 h and then incubated with 300 μM of $ZnCl_2$ for 2 h in serum-free MEM. Treated cells were fixed and the expression of tau phosphorylation was assessed by measuring the levels of immunoreactivity to the phospho-Tau-Ser262 antibody with immunocytochemistry. Bar size = 20 μm.
131x102mm (300 x 300 DPI)

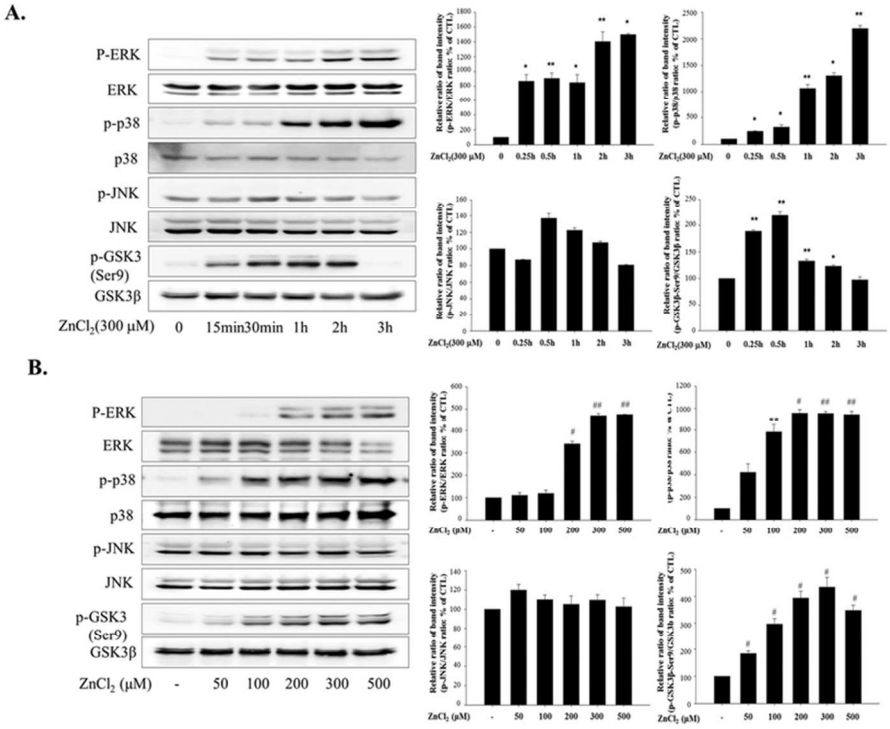

Figure 4. Zinc-induced signaling pathways that phosphorylate tau in rat primary cortical neurons. Rat primary cortical neurons were incubated in serum-free MEM with 500 μM $ZnCl_2$ for varying durations (15 min–3 h) and with increasing concentrations of $ZnCl_2$ (50, 100, 200, 300, or 500 μM) for 3 h at 37°C. A. B. Cells were harvested for western blot analyses, and the activation of ERK, p38, JNK, and GSK3β was assessed by measuring each of the respective phosphorylated forms of these signaling proteins. The total amounts of ERK, p38, JNK, and GSK3β were measured and used as controls. The data represent the mean ± S.E.M. (n = 4). * $p < 0.05$, ** $p < 0.01$ CON vs. $ZnCl_2$.
77x58mm (300 x 300 DPI)

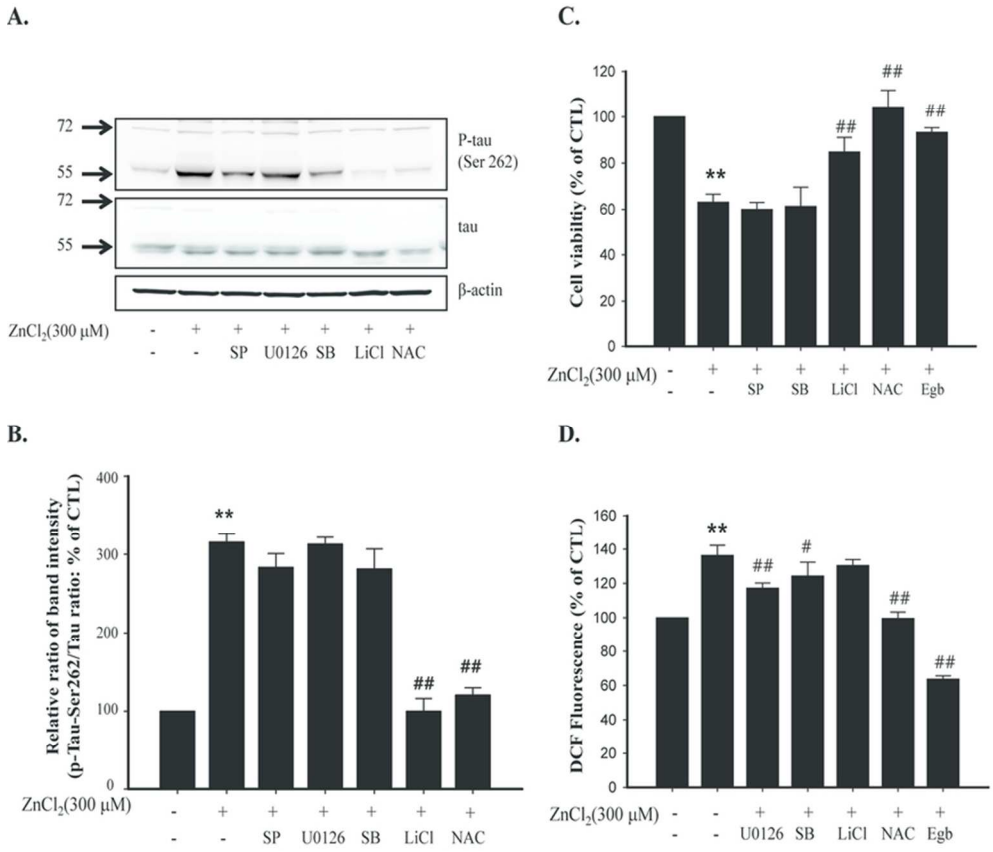

Figure 5. The association of GSK3β activation with tau phosphorylation. Rat primary cortical neurons were pretreated with inhibitors (10 μM SP600125, 20 μM SB203580, 10 μM U0126, 10 mM LiCl, or 1 mM N-acetylcysteine) for 1 h and then incubated with 300 μM of $ZnCl_2$ for 2 h in serum-free MEM (A,B). A. Cells were harvested for Western blot analyses, and the levels of tau phosphorylation were assessed by measuring levels of immunoreactivity to the phospho-Tau Ser262 antibody. Total amounts of tau and β-actin were measured and used as controls. B. The graph shows the densitometric quantification data of the phospho-Tau Ser262 band intensities. Rat primary cortical neurons were pretreated with Egb761 and MAPK inhibitors for 1 h and then incubated with 300 μM $ZnCl_2$ for 2 h in serum-free MEM (C,D). C. Cell viability was measured with a MTT assay. The data represent the mean ± S.E.M. (n = 4). * $p < 0.05$, ** $p < 0.01$, $^{\#}$ $p < 0.005$, $^{\#\#}$ $p < 0.001$. D. Intracellular ROS levels were measured with $DCFH_2$-DA fluorescence (490/530 nm). The data represent the mean ± S.E.M. (n = 4). * $p < 0.05$, ** $p < 0.01$ CON vs. $ZnCl_2$, $^{\#}$ $p < 0.05$, $^{\#\#}$ $p < 0.01$ $ZnCl_2$ vs. inhibitors. The data represent the mean ± S.E.M. (n = 6). * $p < 0.05$, ** $p < 0.01$ CON vs. $ZnCl_2$, $^{\#}$ $p < 0.05$, $^{\#\#}$ $p < 0.01$ $ZnCl_2$ vs. inhibitors.
74x62mm (300 x 300 DPI)

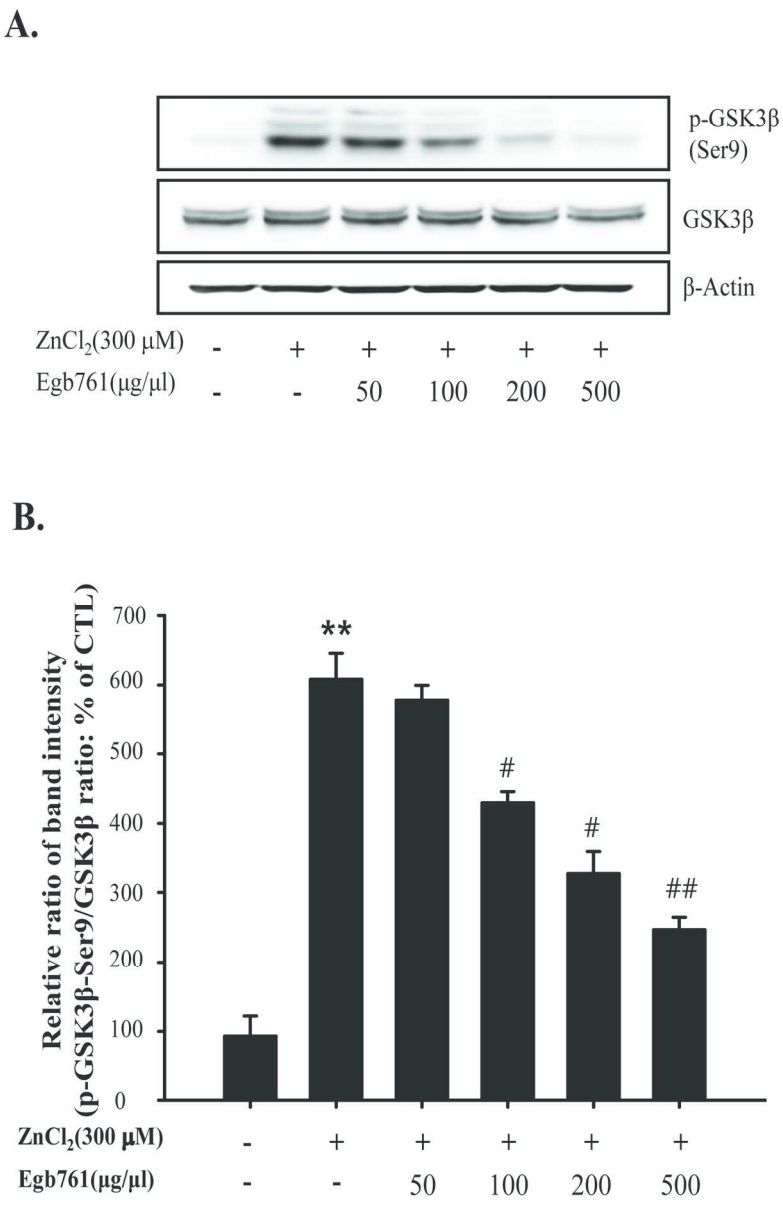

Figure 6. The effects of Egb761 on GSK3β activation in primary cortical neurons. Rat primary cortical neurons were pretreated with Egb761 (50-500 μg/mL) for 1 h and then incubated with 300 μM $ZnCl_2$ for 2 h in serum-free MEM. A. Cells were harvested for western blot analyses, and the expression of GSK3β was assessed by measuring the phospho-GSK3β-Ser9 antibody. Total amounts of GSK3β and β-actin were measured and used as controls. B. The graph shows the densitometric quantification data of the phospho-GSK3β-Ser9 band intensities. The data represent the mean ±S.E.M. (n=6). * $p < 0.05$, ** $p < 0.01$, $^{\#}$ $p < 0.005$, $^{\#\#}$ $p < 0.001$.
67x99mm (600 x 600 DPI)

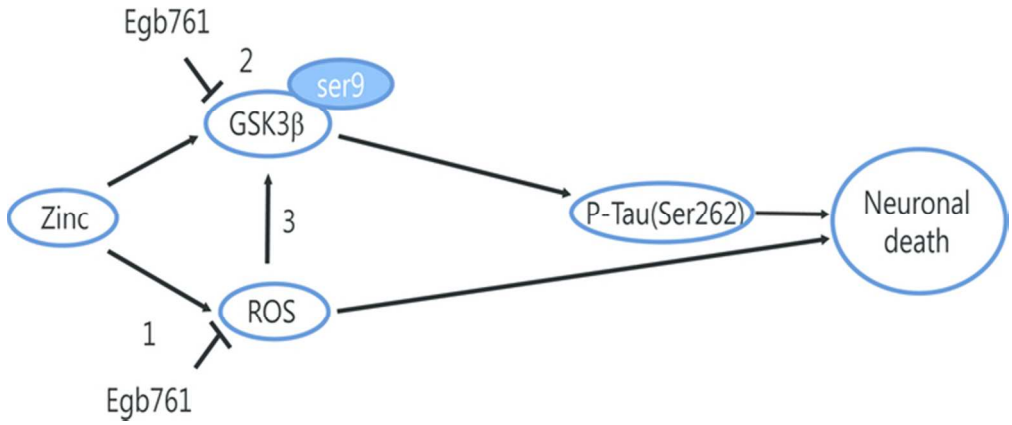

Figure 7. Diagrammatic scheme illustrating the effects of Egb761 in rat primary cortical neurons. Egb761 inhibits tau phosphorylation at Ser262 through 3 pathways: 1. The direct inhibition of intracellular ROS, 2. The direct inhibition of GSK3β phosphorylation, and 3. The inhibition of GSK3β through ROS downregulation.
30x12mm (600 x 600 DPI)